Understanding the impact of cloud microphysics, urbanization, and sea surface temperature on modelling a hail event in Surabaya, Indonesia

F. P. Sari[1,2*], G. J. Steeneveld[1], A. Tsiringakis[1]

[1]Meteorology and Air Quality Section, Wageningen University, Wageningen, Netherlands.

[2]Department of Meteorology, School of Metereology Climatology and Geophysics, Bintaro, South Tangerang, Indonesia.

Key Points:

- Cloud microphysics and urban canopy scheme selection
- Hail occurrence over urban area
- Impact of urbanization and sea surface temperature increase toward thunderstorm-hail event intensity

*Funded by Indonesia Endowment Fund for Education (LPDP)

Corresponding author: F. P. Sari, fitriapsari99@gmail.com

Abstract

In the recent period between 2014 and 2017, five hail events have been reported in Surabaya of which four of them occurred in the urban area. The increasing number of high buildings is the proof of Surabaya government to deal with the urbanization challenge. Although deep convective clouds commonly develop, hailstorm development requires specific conditions. This lead to the question: Is the urbanization the culprit of the recent hail events in Surabaya? An investigation of the 7$^{\text{th}}$ March 2017 hail event has been conducted using the high-resolution Weather Research and Forecasting (WRF) model to answer this question. The study does not only address the effect of urbanization, but also the impact of sea surface temperature and aerosol load to the thunderstorm's dynamic and physics are examined. The combination of Morrison-2 and single-layer urban canopy model was selected as a reference simulation due to the good correspondence of the storm cloud initiation and movement as well as the rain pattern over the city. The low-level convergence creates an instability, while the urban-heat release provides more energy to induce hail formation and retain the thunderstorm's lifetime in the city. The factors contribution to the thunderstorm intensity in analyzed using factor separation method. Both urbanization and SST increase contribute to the enhanced thunderstorm in the city which produces three times stronger updraft, two times more of maximum graupel mass mixing ratio, and finally results 15-30% more accumulated precipitation in the Surabaya urban area.

1 Introduction

Deep convective clouds in the maritime tropical area (i.e Indonesia) commonly develop [*Zipser et al.*, 2006], yet hailstorms are exceptional due to the very specific condition of formation and subsequent development [*Chevuturi et al.*, 2014]. For hail formation, strong vertical wind shear with sufficient moisture load flow is needed [*Orville and Kopp*, 1977; *Chevuturi et al.*, 2014]. Multiple updrafts and downdrafts are also required to produce a hailstone through continuous deposition and shedding of ice particles within thunderstorm developments [*Chatterjee et al.*, 2008]. Nonetheless, in the period of 2014 - 2017 five hail events have been reported in Surabaya [*Ary*, 2017], Indonesia.

Since these hail events are quite new for Surabaya, the dynamics and physics of the thunderstorms are not well understood yet. This leads to the unpreparedness of early warning system and mitigation towards the impacts. As a result, the most recent hail event accompanied by strong wind gust are severe treats for the society. The storm caused damage to public building structures and some vehicles, heavy traffic jam, and falling trees caused some casualty [*Eusabio*, 2017]. Furthermore, instead of forecasting the hailstorm, the weather warning is disseminated by 'nowcasting' [*Adams-Selin and Ziegler*, 2016] because only weather radar can detect this event. Yet, the weather radar does not provide a full understanding of the thunderstorm's physics and dynamic as well as the cause of the thunderstorm intensity increase. Therefore, this study utilizes a numerical weather prediction technique to bridge this gap knowledge.

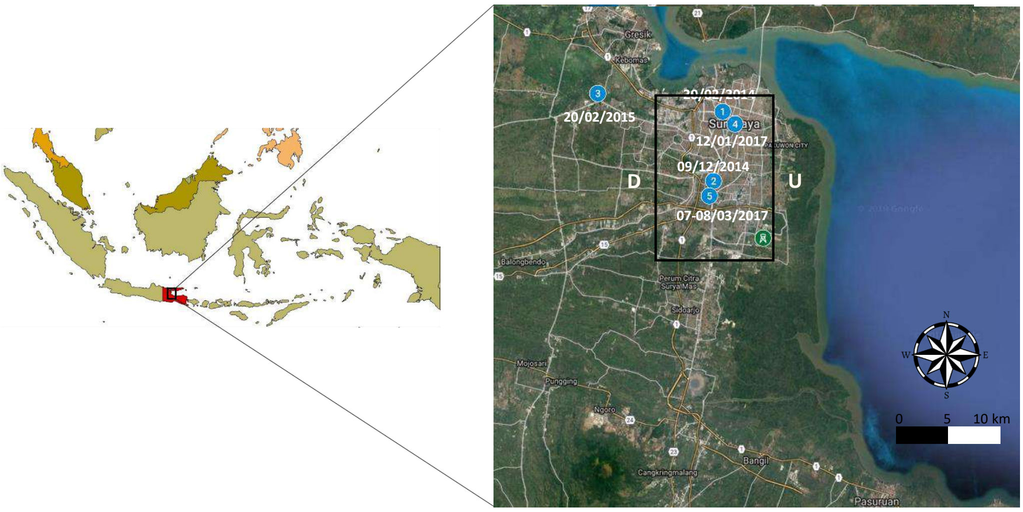

Figure 1. The location where hail event reported in Surabaya as well as the study area of this current study in Indonesia big map; Blue and green marks indicate the area where hail event reported as its sequence of occurrence and the location of Automatic Weather Station, respectively. The open black rectangle displays the defined urban sector with upwind (downwind) area indicated by U(D) alphabet.

Nevertheless, forecasting thunderstorm is still a challenging task in the field of numerical weather prediction (NWP)[*Halder et al.*, 2015]. The interaction of convection and microphysics in the convective cloud development has been proven as the main factor in the success or failure of NWP [*Stensrud et al.*, 2015]. Moreover, latent heating in cloud microphysics because of condensation, freezing, and deposition plays an important role in the development of convective systems [*Hazra et al.*, 2013]. Due to the great contribution of cloud microphysics to convective cloud modelling, the sensitivity of cloud microphysics scheme during hail event simulation should be accounted for. Thus, to the author's knowledge, this is the first study that investigates vigorous thunderstorm during hail event related to cloud microphysics using the high-resolution model in Indonesia.

Furthermore, urbanization is expected to continue in the next decades including Surabaya as the second largest city in Indonesia [*Tjiptoherijanto*, 1999]. The change of land use land cover (LULC)[*Sobirin and Fatimah*, 2015] and the rapid growth of high buildings and/or apartments [*Salanto*, 2015] are proofs of Surabaya government's attempt to meet housing needs in the city [*Pemerintah Walikota Surabaya*, 2014]. The fact that most of the hail events reported in Surabaya urban area (Figure 1) [*Ary*, 2017] deduce a hypothesis that the presence of urban area induce the vigorous thunderstorm. Some studies also found that three mechanisms associated to urban aspects; (i) urban heat island (UHI)[*Lin et al.*, 2011], (ii) the roughness effect of urban surface [*Li et al.*, 2013], and (iii) urban aerosol effects [*Yang et al.*, 2017], can trigger stronger convective cloud formation [*Han et al.*, 2012], increase precipitation rate over and downwind of the urban area [*Gunst*, 2016], and modify the regional precipitation pattern [*Li et al.*, 2013]. In addition, the increasing frictional drag in the rougher terrain of the urban surface can enhance the flow convergence in the city [*Bornstein and Lin*, 2000]. The accumulating urban aerosol which functioned as cloud condensation nuclei (CCN) also can intensify the condensation process in cloud microphysics during cloud development [*Yang et al.*, 2017]. Moreover, the increasing sea surface temperature (SST) in Madura Strait is suspected to contribute to the thunderstorm, since most of the cloud development originates there [*Sari*, 2014]. Therefore, the impacts of urbanization and SST increase on the hail event need to be understood and this study will investigate urban-induced hail event in Indonesia, particularly Surabaya. With these considerations, the purposes of this study are listed: (i) to evaluate the skill and the sensitivity of cloud microphysics and urban canopy scheme's combination of the high-resolution model to simulate hail event, (ii) to study in detail the thunderstorm's dynamics and physics during hail event simulation using the most appropriate combination of cloud microphysics and urban schemes, and (iii) to understand the impact of urbanization and SST increase towards the thunderstorm intensity.

This study is organized as follows: section 2 describes a brief overview of the selected case study, section 3 depicts model configuration and experimental design, section 4 shows the results of model performance and baseline run selection, section 5 presents the detail investigation of thunderstorm's dynamic and physic of selected case study using the baseline run, section 6 delivers analysis of the influence of urbanization and SST factors to the intensity of thunderstorm over Surabaya urban area. Lastly, conclusions are drawn in Section 7.

2 Case description

This study performs a real case simulation of the 7^{th} March 2017 hail event in Surabaya. The vigorous thunderstorm was reported hit Surabaya urban area at 15.50 LST (Local Standard Time = UTC+7) [*Hermawan*, 2017]. In the meantime, the westerly monsoon was active in Indonesia, carrying moist mass air from the Indian Ocean, including Surabaya. Yet, the storm was observed by the Doppler Weather Radar (DWR) had opposite direction to this main synoptic wind flow (Figure 2a). This indicates that the local scale of sea breeze occurrence (Figure 2b) dominating the storm development and movement as the typical convective cloud growth over this area [*Sari*, 2014]. The vigorous thun-

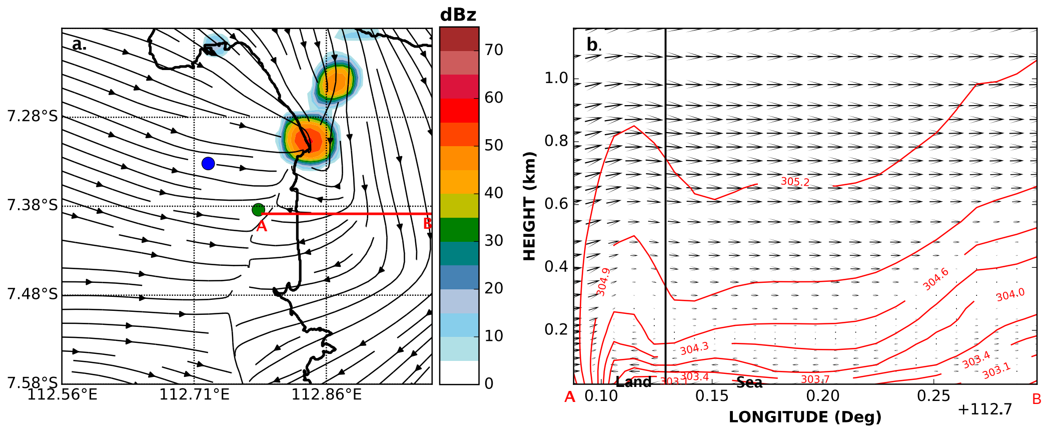

Figure 2. a.The first occurrence of modelled storm cloud echoes on column-maximum reflectivity on 7^{th} March 2017 at 14.20 LST. Blue (green) dots indicates the observed hail occurrence (Juanda Meteorological Station (JMS)) location; b.The modelled cross-section of zonal-vertical flow at 10-meter (u-w; vector) and potential temperature (θ; contour) at 30 minutes before the cloud storm development indicating sea breeze occurrence in the surface (at 13.50 LST). The x-axis corresponds to a red horizontal line in Figure 2a.

derstorm development is quite fast. The first cloud echo swiftly appeared on the JMS

DWR screen at 14.41 LST in the eastern part of Surabaya coastal area with core reflectivity of 55 dBz. About 40-minutes after its initiation, this cloud headed to a southwest part of the Surabaya urban area. It reaches its highest reflectivity of 65 dBz while passing the urban area from 15.41 to 16.01 LST and should be responsible for the hail event occurrence. However, an early morning sounding (07.00 LST) taken at JMS observatory showed a stable layer from 925 hPa level (not shown). The Convective Available Potential Energy (CAPE) was only 763 J/kg, indicating atmosphere marginally unstable. Yet, it has not been categorized has a high possibility to develop vigorous thunderstorm in Surabaya according to Taruna's study about the possibility of cumulonimbus cloud and thunderstorm development using Radiosonde in Surabaya [*Taruna et al.*, 2016]. A severe cumulonimbus producing hail in Surabaya occurred when CAPE is about 901 - 1669 J/kg in the morning (before the hail event occurrence)[*Tresnawati*, 2016]. Whilst, the night sounding of 7$^{\mathrm{th}}$ March 2017 showed an unstable layer from 900 to 750 hPa, indicating that the middle layer atmosphere was still unstable as the remaining of the storm presence. Unfortunately, there were no soundings in between, revealing an incomplete investigation of the storm development. Therefore, due to the greatest impacts yet the lack information of the hail formation during this typical thunderstorm, suggesting the 7$^{\mathrm{th}}$ March 2017 hail event is suitable to conduct in this study.

3 Methodology

3.1 Model configuration and data

The Advanced Weather Research and Forecasting (WRF-ARW) model version 3.7.1 is employed to reach the study aim. WRF is a non-hydrostatic model combined with ARW dynamics solver which comprise physics schemes, numeric/dynamics options, and some packages that allow the users to modify these options as their preferences [*Skamarock et al.*, 2005]. In this study, all simulations used three nested domains of 25 km, 5 km, and 1 km horizontal resolutions. The number of grid points are 51 x 51 for each domain with the JMS location set as the centre of the domains (Figure 3a and Table 1). The highest resolution of 1-km spatial and 10-minutes temporal of the innermost domain follow previous studies which succeed carry out the hail event simulation within this range [*Chevuturi et al.*, 2014; *Luo et al.*, 2017]. The model uses 45 levels of hydrostatic vertical pressure, with about 25 layers located below 1.5 km above the ground. The model top is 100 hPa and the lowest level set at about 30 m above the surface to prevent instability on the urban canopy model (UCM) scheme when the average building height (ZR) is modified.

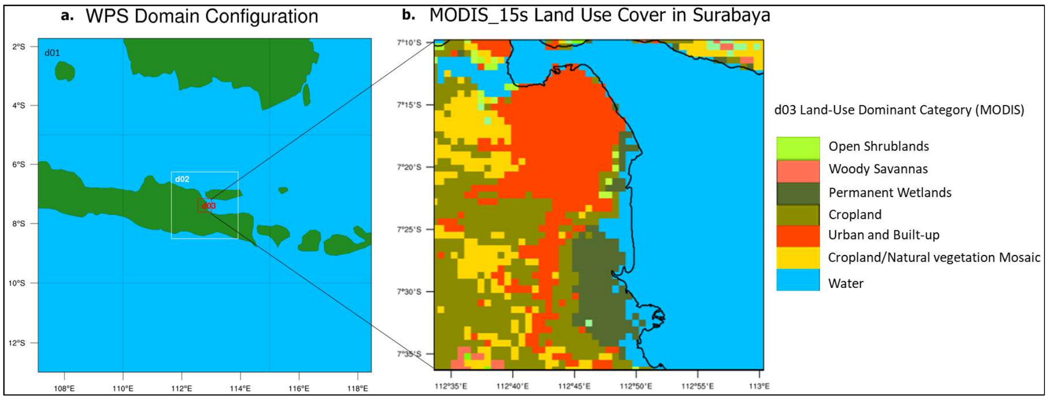

Figure 3. (a) WRF Model domain and (b) LULC dominant category of the innermost domain

All simulations are integrated for 48 hours, starting from 6$^{\text{th}}$ March 2017 at 19.00 LST. In total, 12 hours for spin-up time and 36 hours the remaining data are used for verifying and analyzing the thunderstorm. Three operational analysis dataset of 0.25° European Centre for Medium-Range Weather Forecasts (ECMWF), 1° ECMWF, and 1° National Centers for Environmental Prediction (NCEP) were tested beforehand. Results demonstrated that WRF can simulate the vigorous thunderstorm reasonably using 0.25° ECMWF compared to other datasets (i.e forceful updraft, stronger convergence, higher surface-CAPE number). The finer resolution of ECMWF dataset also able to simulate the similar length of the thunderstorm lifetime with clearly updraft and downdraft side by side (result not shown). Hence, the 0.25-degree resolution and six hourly updated of ECMWF dataset are used as the initial and lateral boundary condition for this study. The surface weather variables (i.e 10-meter wind, 2-meter air and dew-point temperature) of automatic weather station (AWS), soundings observation, and JMS DWR (i.e reflectivity and accumulated precipitation) are used as corresponding observational data. This simulation used a 15-seconds resolution of MODIS LULC due to its consistency of the urban area size yet only one urban area category is treated, a high-density residential (Figure 3).

Table 1. Overview of model and parameterization option in the 7th March 2017 hail event

Model	WRF Version 3.7.1
Map Projection	Mercator
Horizontal resolution	Nested domains of 25, 5, and 1 km
Vertical resolution	45 levels with 100 hPa of model top
Central point of domains	JMS point observation (7.384°S, 112.783°E)
Radiation	Dudhia for shortwave, RRTM for longwave
Land Surface Model	a unified Noah (Noah LSM)
Planetary Boundary Layer	Yonsei University (YSU)
Cumulus parameterization	Kain-Fritsch (used only in 1st and 2nd domain)
Cloud Microphysics	Single moment of Goddard Cumulus Ensamble with hail option (Goddard)
	Single moment of New-Thompson scheme, but ice and rain water in double moment (Thompson)
	Double moment of Morrison-2 (Morrison)
Urban Canopy Model	No UCM (SLAB)
	Single Layer UCM (SUCM)

3.2 Experimental design

There are three stages of data analyzing to address the threefold detailed purposes. Two experimental designs have been developed to: (i) obtain a baseline run (CNTL) of the most appropriate combination of microphysics and urban parameterization; this will be used for further investigation of the thunderstorm and (ii) modify the urban surface representation and SST using the CNTL run as a reference. In the first experiment, six model runs are considered (i.e. combination of three microphysics and two UCM schemes), while the second experiment explores scenarios for urbanization and SST increase.

To understand the microphysical process as well as the effect of the city on the hail formation, a comparative simulation is performed using three microphysical schemes and two UCM schemes. These three microphysics schemes include two popular bulk micro-physics schemes which successfully simulate tropical deep convection [*Stanford et al.*, 2017]:

(i) The New-Thompson (Thompson) [*Thompson et al.*, 2008], (ii) the Morrison-2 (Morrison) [*Morrison et al.*, 2005], and one single-moment with hail option which succeeded on simulating hailstorm in India [*Chevuturi et al.*, 2014] and Sydney [*Benjamin*, 2015], namely (iii) the Goddard Cumulus Ensemble (Goddard)[*Tao et al.*, 2003]. They compute at least same six hydrometeor particles of water vapour, cloud water, rain water, snow, cloud ice, and the third class of ice (can be graupel or hail). Whilst, the importance of the use of urban physics schemes is evaluated by (i) switching off the UCM (SLAB) and (ii) activating the single-layer UCM of WRF model (SUCM). By implementing SUCM, all urban effects are vertically treated to be sub-grid scale in which all urban processes are considered to occur below the lowest eta level. This scheme is known as a fairly sophisticated manner to mimic a wide range of urban processes [*Kusaka and Kimura*, 2004] which includes the influence of (i) street canyons parameterization, (ii) building shadowing and radiation reflection, and (iii) roof, wall, and road heat fluxes based on thermodynamics[*Kusaka et al.*, 2001]. During the sensitivity assessment, for each microphysics and urban parameterization used their default settings and no attempt has been made to modify or fine-tune beforehand.

Table 2. Summary of second experiment design.

Experiment	**SST** (°C)	**Building Height** (m)	**CCN Concentrations** (cm $^{-3}$)
CNTL	default	default	default
SST3.0	+3.0	default	default
ZR25	default	25	default
CCN4000	default	default	4000
SST3.0ZR25	+3.0	25	default
SST3.0CCN4000	+3.0	default	4000
ZR25CCN4000	default	25	4000
SST3.0ZR25CCN4000	+3.0	25	4000

For the second modelling experiment, the SST threshold follows SST data analysis which derived from the monthly average of the ERA-Interim-40 dataset. It shows that SST in the Madura Strait already increased 1.5°C with a positive trend (y = 0.0031x + 28.111) in the last thirty years during the wet season (figure not shown). Therefore if we assume that SST will linearly increase, in the next 30 years the SST can reach up to 3.0°C. However, in this study, we did not increase the water vapour in the atmosphere since they are unlimited under westerly monsoon due to a moist mass air coming from India Ocean. Therefore, the SST increase is expected to be a driver of the cloud formation as the local circulation of sea-breeze promotes water vapour to the inland.

Whilst, the default building height (ZR) setting is 7.5 m for the high-density category. The change of this parameter follows the regulation of Surabaya government [*Pemerintah Walikota Surabaya*, 2014] which says that the allowed height for housing/private building is only 3 - 5 meters/floor. However, the current situation of Surabaya average building height is 2 - 3 storeys in which the average building height is about 6 - 15 meter. Therefore, the high scenario of ZR for residence is assumed to be 25 m and can only be higher if it is for commercial purposes [*Pemerintah Walikota Surabaya*, 2014]. Finally, the CCN number permutation follow the scenario of *Han et al.* [2012] who also investigated the urban aerosol impact on an idealized deep convective cloud. The CCN concentration of 4000 cm^{-3} set as the threshold of the high scenario.

The factor analysis technique of *Stein and Alpert* [1993]; *Rozoff et al.* [2003] is used to find which process is dominant among three factor influence. Because of three-factor variations are considered (i.e SST, ZR, and CCN), eight simulations (include CNTL) must be carried out (Table 2). The denoted term, as well as the difference fields necessary calculation using that technique, are listed in Table 3. It should be noted that attention is not only paid to individual factor but also the contribution of interacted factors since in real condition it is difficult to separate one to other.

4 Model performance and baseline run selection

This section compares the results of the model simulation with observations. It will provide a general overview of the WRF model performance as well as the sensitivity of the thunderstorm to the microphysics and urban physics scheme used in the model. First, the performance of the model to simulate atmospheric vertical profile in the morning before thunderstorm growth is assessed. Afterwards, a verification of the cloud microphysics scheme on simulating 6-h accumulated precipitation during thunderstorms will be per-

Table 3. Summary of denoted terms and the difference field mechanism of factor separation analysis.

Term	Difference	Mechanism
CNTL	CNTL	Baseline run
SH	SST3.0 - CNTL	SST
ZH	ZR25 - CNTL	Building height
CH	CCN4000 - CNTL	CCN concentration
SHZH	SST3.0ZR25 - (SST3.0 + ZR25) + CNTL	SST and building height interaction
SHCH	SST3.0CCN4000 - (SST3.0 + CCN4000) + CNTL	SST and CCN concentration interaction
ZHCH	ZR25CCN4000 - (ZR25 + CCN4000) + CNTL	Building height and CCN concentration interaction
SHZHCH	SST3.0ZR25CCN4000 - (SST3.0ZR25 + SST3.0CCN4000 + ZR25CCN4000) + (SST3.0 + ZR25 + CCN4000) - CNTL	Interaction of all factors

formed. Finally, the importance of applying the UCM to obtain the model results closer to the observation will be discussed. Indeed, assessing the urban scheme will only work with the selected microphysics from previous verification step. The best combination of microphysics and urban canopy scheme will then be chosen as a baseline run considering to the closest value and pattern of spatial accumulated precipitation and statistical number of weather variable observation.

4.1 Atmospheric vertical profile

The modelled and observed JMS sounding data at 07.00 LST and model output for different ensemble schemes shown in Figure 4. In general, it shows that vertical atmospheric profile is well simulated yet there is some bias in a certain level of each vari-

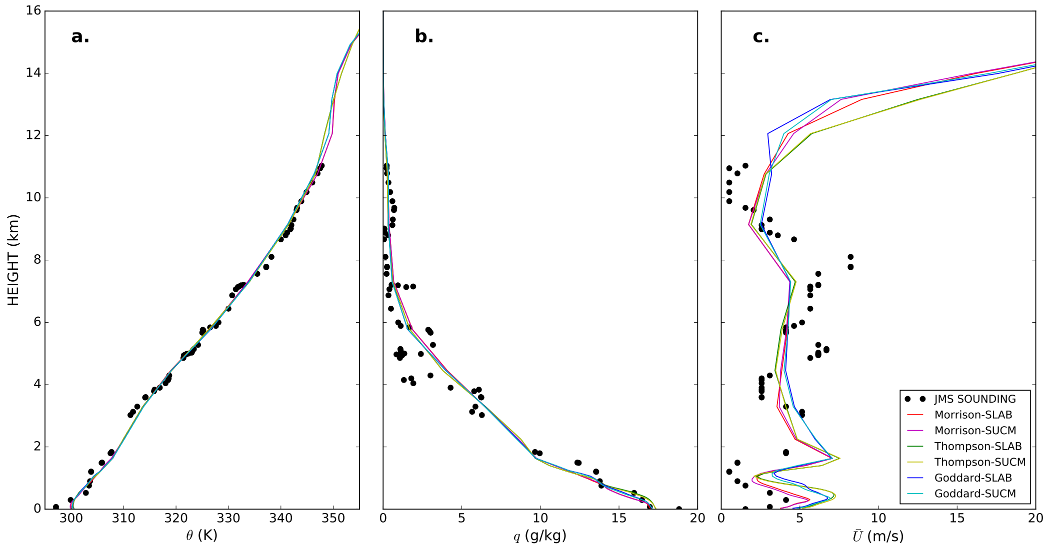

Figure 4. Modelled (color line) and observed (black dot) vertical profile of a. potential temperature (θ; K), b. specific humidity (q; g/kg), and c. horizontal wind speed ($\bar{U}$; m/s). Sounding taken at JMS point observation on 7$^{\text{th}}$ March 2017 at 07.00 LST.

able. For instance, the model produces a warm bias of potential temperature (∼1-2 K) from the surface to the height of 4 km and cannot capture the temperature inversion at the lowest level (z∼0.6 km) (Figure 4a). The missed inversion is because the model has a coarse initial condition compared to the observation. The model also tends to underestimate the specific humidity in the low level (∼2 km) and overestimate in the upper air (Figure 4b). The moister layer of the sounding profile observation by ∼ 1-1.5 g/kg in the surface indicates that the real atmosphere contains much more water vapor due the closer of point observation to the body water. Furthermore, the modelled near-surface wind speed is overestimated by ∼2-3 m/s, which agrees with the findings of *Kilpeläinen et al.* [2012] who found that the modelled low-level jet (LLJ) was deeper and stronger than the observation. Surprisingly, the pattern and the height of maximum wind which located at ∼280 m is in a good agreement to the observation (Figure 4c) since normally models have difficulties to capture this LLJ feature [*Dutsch*, 2012; *Gevorgyan*, 2018]. Although the model does a good job in the vertical atmosphere simulation, this analysis seems not sensitive to the use of different microphysics schemes. The difference among the schemes are very small and only Morrison which looks slightly closer to the observation when simulating vertical profile of wind speed. This difference on the simulated wind speed can be related to the difference of simulated downdraft strength among the schemes in which influenced by the parameterization of precipitation evaporation [*Rajeevan et al.*, 2010]. Therefore, a comparison of simulated accumulated precipitation among the schemes is needed to understand this microphysics sensitivity.

4.2 Accumulated precipitation field

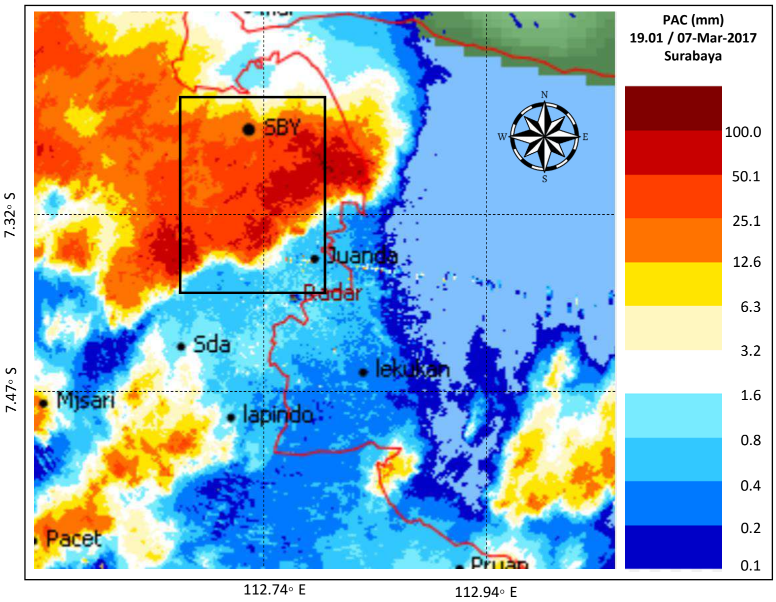

Figure 5. The 6-hour (6-h) accumulated precipitation of DWR JMS PAC product (mm) on 7$^{\text{th}}$ March 2017 at 19.00 LST (Source: *Ary* [2017]).; black box indicates Surabaya urban area.

Figure 5 presents the 6-h accumulated precipitation field derived from precipitation accumulation (PAC) of the JMS DWR product. The PAC product is generated from 13.00 to 19.00 LST by converting radar reflectivity to rain using Z-R relationship [*SELEX*, 2007]. This conversion may lead to the uncertainty of the precipitation value due to the variability of raindrop size distribution during a rainfall event [*Alfieri et al.*, 2010], but it is still useful to verify the rain pattern spatially. From this figure it is shown that the most precipitation is elongated from eastern coastal area to the southwest of Surabaya urban area and exceeds 50.1 mm. This elongated pattern of the high precipitation area is well simulated by the model (Figure 6), yet slightly shifted to the sea compared to observation. This pattern can be seen in all schemes although the area of the maximum values tend to be somewhat narrower. This can be explained by the model's coarser resolution (i.e the model has a 1-km resolution while the radar has 200-m).

Despite the model shows a bias in the location of accumulated precipitation, among the microphysics schemes, Morrison shows the best agreement of the elongated precipitation peak and pattern (Figure 6a-b). The qualitative precipitation forecast also concurs to the observation, which exceeds 50 mm. Although Thompson also produces the same amount of the highest precipitation, it overestimates the rain area coverage (Figure 6c-d). This because Thompson tends to generate more small raindrops on higher number concentrations (Figure A.1c-d) in which increasing rain production (Figure A.2c-d). The extensive area of the rain production not only leads to an increased latent cooling (especially from the surface to the height of 1.6 km) but also enhances the cover area of precipitation. The cold pool is somewhat stronger than Morrison producing wider rain area coverage more eastward over the sea (Figure A.2c-d). This finding contradicts to the result of *Stensrud et al.* [2015] which stated that Thompson has no coherent special bias due to the weaker cold pools intensity. Yet, it confirms the previous study of another hail event in Surabaya [*Sari*, 2017] that Thompson tends to develop thunderstorm too far from observation and wider cloud areal coverage. Among two others, Goddard single moment is the poorest scheme on producing rain mass (Figure A.1e-f), even the latent cooling is lower compared to another microphysics scheme (not shown). This scheme produces the least 6-h accumulated precipitation as well as the narrowest of precipitation spatial coverage (Figure 6e-f).

4.3 Surface parameter analysis

A point-to-point comparison of the surface variable between JMS AWS observation and WRF output for the use of urban physics schemes is shown in Figure 7. Here, the comparison only includes the Morrison microphysics scheme, since this scheme can simulate better than the others in terms of vertical profiles and accumulated precipitation field. Generally speaking, WRF can reproduce surface variable fluctuations as observations, though there is bias for each variable. The model seems producing a higher 2-meter dew point in the morning compared to observation (Figure 7b) which can help to provide a fuel for thunderstorm development in the afternoon. This higher moisture can be related to the ECMWF operational analysis as a forcing data which provides higher water vapour content in the low level compared to NCEP dataset (not shown). The short occurrence of the sea breeze, indicated by the change of westerly to the easterly wind

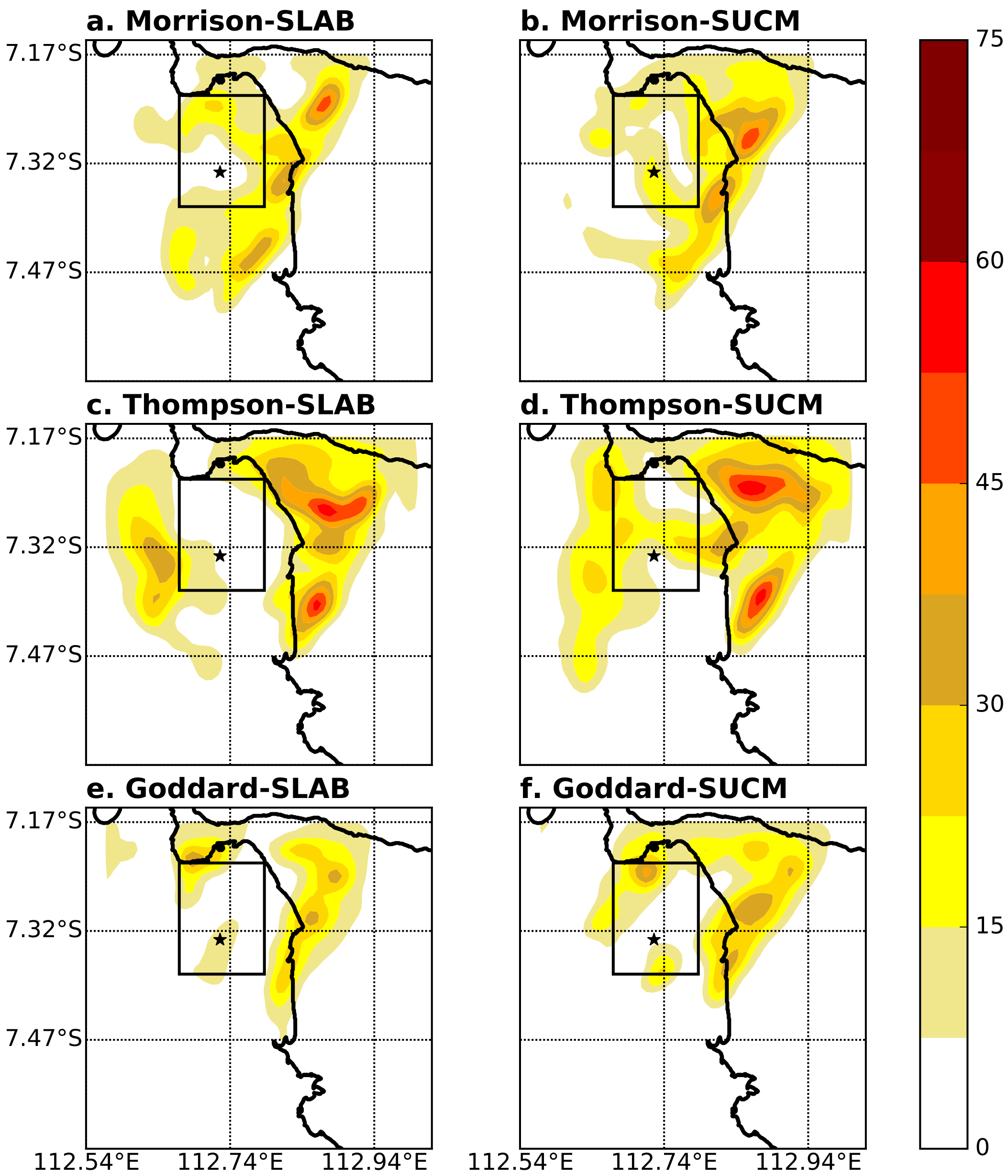

Figure 6. Simulated 6-h accumulation precipitation field for different ensemble scheme; the small black star indicates the location where hail accompanied by heavy rain reported on 7[th] March 2017 from 13.00 to 19.00 LST.

from ~14.00-16.00 LST is also well reproduced although this is lagging 30 - 40 minutes behind the observation (Figure 7d).

Overall, the use of a UCM can decrease the bias for each variable except for wind direction. For temperature and surface dew point depression, the UCM reduces the bias

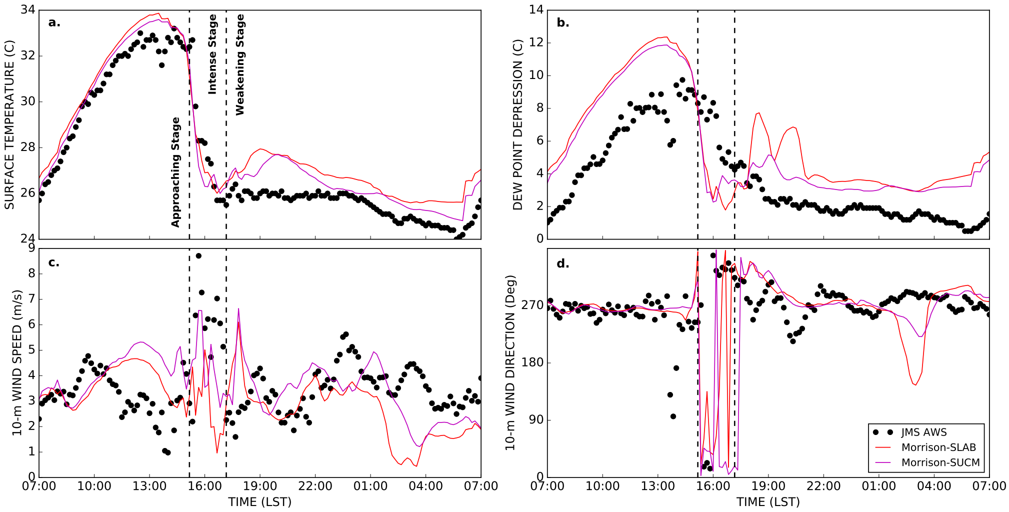

Figure 7. Time series of modelled (colour lines) and observed (black dot) surface variable of a. 2-m temperature, b. 2-m dew point depression, c. 10-m wind speed, and d. 10-m wind direction of JMS AWS. The vertical dashed line indicates the stage of the thunderstorm's life cycle on the day when hail event occurred over the Surabaya urban area according to the DWR JMS.

substantially from 0.89° to 0.58°C and from 2.25° to 1.74°C respectively. The greater bias reduction of dew point depression can be seen clearly after thunderstorm weakening (Figure 7b). The observations show a moister surface layer after thunderstorm occurrence while both schemes are slightly drier in the lowest level of the atmosphere. However, the SUCM produces a moister layer in the low level compared to the SLAB scheme. This because SUCM calculates vegetation as well as anthropogenic latent heat [*Kusaka and Kimura*, 2004] which results higher latent heat flux over the urban area compared to SLAB scheme (figure not shown). It also stores more heat in the building which leads to the less available of sensible heat flux to heat the air. Thus it is expected that the 2-meter air temperature in SUCM become lower and moister than SLAB scheme. Despite the wind speed has the greatest bias reduction when the UCM is applied (∼45%) (Figure 7c), the correlation of either wind speed or direction is somewhat lower compared to the SLAB (not shown). However, the quick change of wind direction is well simulated under the stronger wind speed (≥3 m/s)(Figure 7c) which implies that WRF is more capable reproducing wind direction for relatively high wind speeds. This is consistent with findings of *Papanastasiou et al.* [2010] that WRF performs poorly on wind direction under low wind speed conditions where the difference mean bias of wind direction between his and this study is relatively similar, 33° and 38° respectively.

By considering the performance of ensemble microphysics and urban physics scheme in comparison to observations, a baseline run for the simulation and modelling of the hail event has been formulated. The combination of Morrison and SUCM scheme show more reasonably performance than others. Hence, this ensemble scheme will be the control run (CNTL) in the next analysis.

5 Simulated thunderstorm in CNTL run

5.1 Simulated spatial reflectivity

Figure 8 shows the simulated spatial of column-maximum reflectivity from the radar observation and the CNTL run. The figure displays the stage of the thunderstorm from approaching to weakening while passing the urban area both in the observation and the simulation field. The approximately 20 - 30 minutes time lag for each stage is shown to commit the delay between the radar observation and the simulation. This time offsetting is due to the delay of the sea breeze occurrence and the lower wind speed generated by the model compared to the observation (Figure 7). Although CNTL produces the 6-h accumulated precipitation pattern and a maximum value closer to the observation, it tends to produce wider clouds and more scattering on the simulated cloud main echo. However, the highest reflectivity when it passes the urban area corresponds quantitatively with the observed value of 55-60 dBz. This value corresponds to the observed maximum reflectivity in the thunderstorm mature stage and should be responsible for the stage where thunderstorm on its most intense stage. The ∼6 m/s westward movement of the thunderstorm is also well simulated in this CNTL field. Furthermore, the model is able to simulate the breakup of cloud storms over the urban area (Figure 8g-h) in which also shown by radar observation (Figure 8c). This findings is consistent to *Zhang et al.* [2017] who also found that the large surface drag force of the presence of urban area induced the storms to bifurcate in the upwind direction of the city. As a result, the accumulated precipitation is much more around the urban and the downwind area than in the city (Figure 5 and 6b). Due to the agreement of the highest reflectivity number as well as the westward propagation on this simulated field, therefore the dynamic and cloud microphysics for each stage of the simulated thunderstorm will be analyzed in detail below.

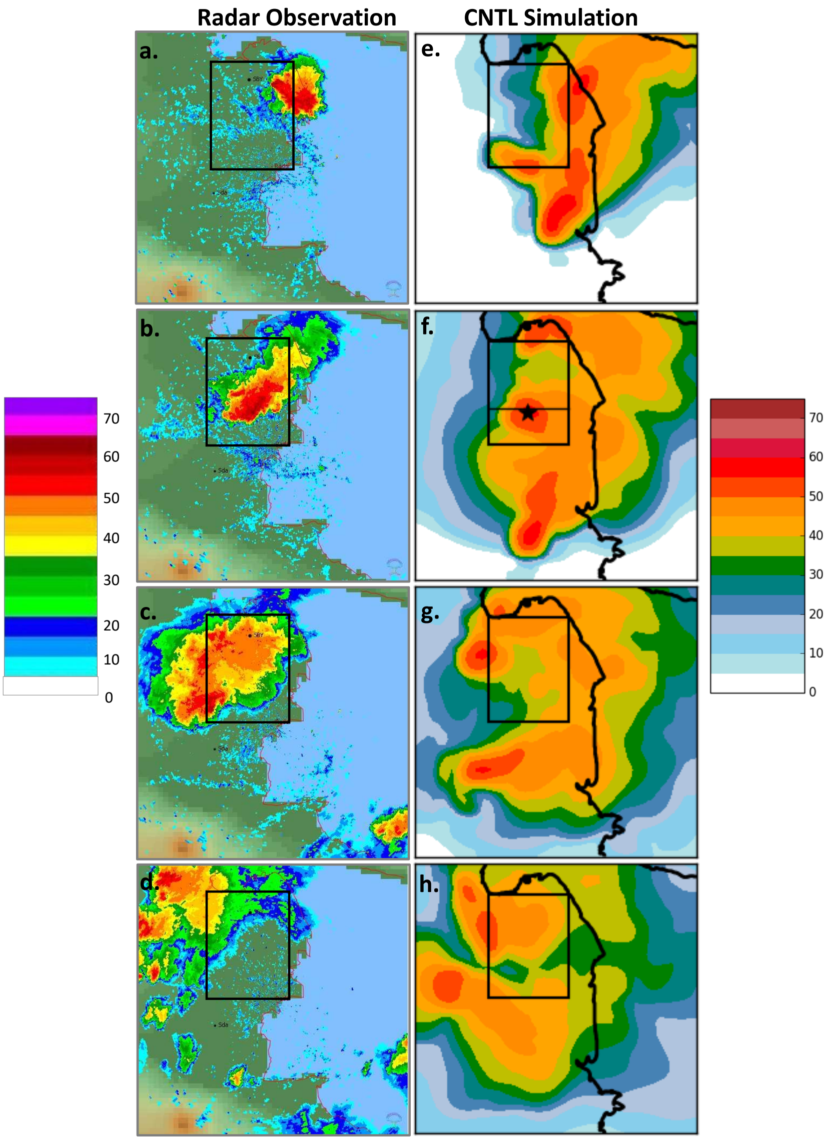

Figure 8. Column-maximum reflectivity field from JMS DWR observation (a-d) and CNTL simulation (e-h) for each stage of the thunderstorm's life cycle. The JMS DWR are from 15.10 to 17.10 LST at 40 minutes interval while the simulated at e. 15.40, f. 16.10, g. 16.50, and h. 17.30 LST, taking into accounts the time errors of the CNTL simulation compared to JMS DWR observation. The black rectangles indicate Surabaya urban area, the horizontal black lines correspond to the location of the cross-section for Figure 10-11, while the small black star at 16.10 LST (f) indicates the location where the hail event reported.

5.2 Simulated cross sectional reflectivity, upward motion, and hydrometeor field

Given the reasonable reflectivity field in the simulation, further analysis of the thunderstorm related to its dynamic and microphysical field will be performed. The investigation considers to the vertical reflectivity, upward motion and hydrometeor field during the evolution of the storm while passing the urban area. The selected time analysis for each stage of the thunderstorm's life cycle is based on the averaged urban area of maximum vertical graupel mass flux time series, in order to examine the hail development.

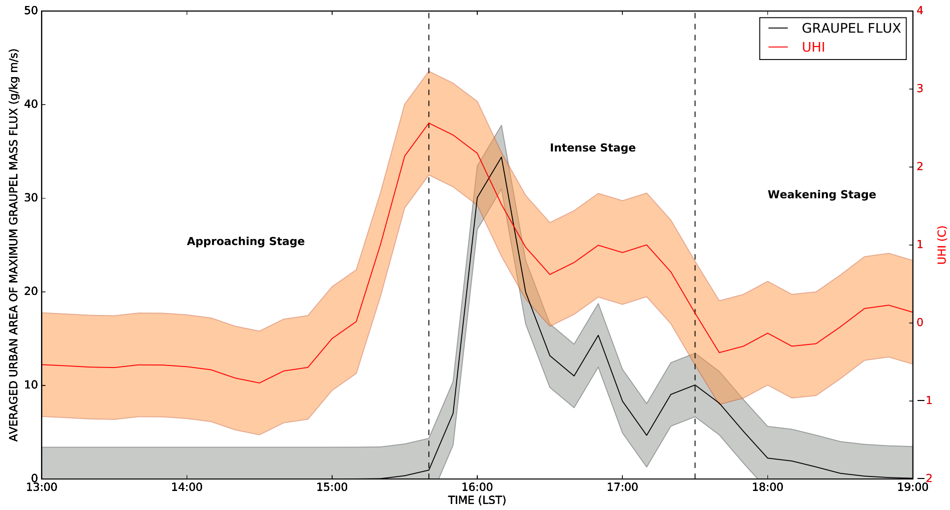

Figure 9. Time series of average (line) and standard deviation (shaded) of the maximum graupel mass flux (black) over the urban area and UHI (red) derived from the difference of mean temperature between urban and the JMS station as rural area during the thunderstorm movement in the CNTL simulation. The urban area averaged based on the black rectangular shape in Figure 8.

Figure 9 enables us to distinguish the thunderstorm evolution while passing the urban area; the approaching stage started at 15.20 LST, the intense stage occurred from 15.40 to 17.30 LST with two peaks before weakening and leaving the urban area from 17.30 LST onward. During the approaching stage, the 1 g/kg m/s of graupel flux indicates the small cloud echo starts to enter the eastern part of the urban area. The rapid increase of the graupel flux occurs after the thunderstorm approaches the urban area in the first twenty minutes. The flux reaches 35 g/kg m/s within 30 minutes, indicating that the thunderstorm is on marginal lightening conditions [*Creighton et al.*, 2014]. Besides the sharp increase of the graupel flux, there is one other smaller peak in the intense stage. This implies that the mature thunderstorm lasts longer in the urban area, the reason of this retained intense stage will be discussed later. In total, the simulated thunderstorm's lifetime over the urban area lasts approximately 1 hour and 50 minutes.

The approaching stage is marked when the graupel flux slightly increases over the urban area (Figure 9). The release CAPE of 2832 J/kg at 15.10 LST along with the low-level moisture incursion at 1.5 - 2 km above the surface (figure not shown) revealing the low-level instability promotes the storm development. Therefore, the sudden 45 - 50 dBz of first cloud echo appears along the coastal line at 15.20 LST and starts approaching the eastern part of the city 20-minutes afterwards (Figure 10a). At this time, the low-level convergence triggers wind shear at ∼250 m above the surface and ∼4 km in the front of the cloud storm, yet the maximum updraft is relatively weak (<5 m/s)) in the city. However, the stratified low-cloud already has a base of ∼800 m in the entire urban area, while rain mass mixing ratio is somewhat low (∼1.0 g/kg) at this time (Figure 11a).

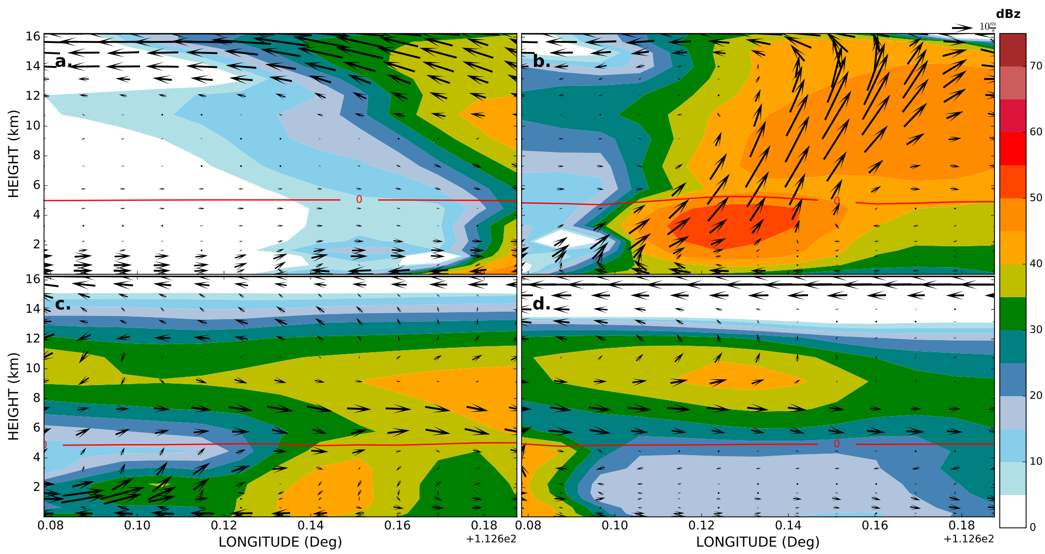

Figure 10. Vertical longitude cross-section of reflectivity fields (shaded; dBz), u-w component wind (arrows; m/s), and 0°C temperature level (red line) of each stage on 7^{th} March 2017 at a. 15.40, b. 16.10, c. 16.50, and d. 17.30 LST. The x-axis corresponds to the Surabaya urban area as shown as a black open rectangular in spatial figure.

The two peaks shown in Figure 9 indicate the mature stage of the thunderstorm. The most intense stage occurred at 16.10 LST and the second one was about 40 minutes later. Looking into the thunderstorm dynamic in the most intense stage, within 30 minutes from its approaching, the main echo of cloud storm only propagates ∼5 km westward. This indicates that the storm movement is somewhat slow. Consequently, the storm is more affected by the urban area while passing, in which results the longer lifetime and the stronger updraft. The delayed of the maximum graupel flux with respect to the maximum UHI timing (Figure 9), however, implies that the city contributes to the vigorous thunderstorm development due to the urban-heat release. As a result, the rise of warm air parcels in the city leads the graupel production to reach its peak about 30 minutes afterwards.

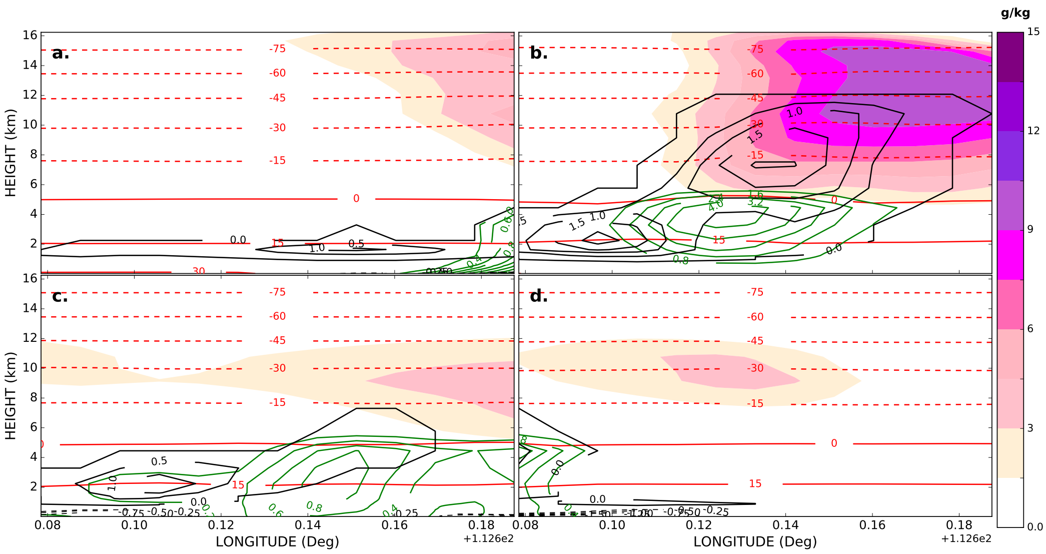

Figure 11. Vertical longitude cross-section of graupel (shaded; g/kg), rain (green; g/kg), liquid water (black; g/kg) mass mixing ratio, negative perturbation potential temperature (dashed black line; K), and temperature (red line; C) for each stage on 7th March 2017 at a. 15.40, b. 16.10, c. 16.50, and d. 17.30 LST in the city. The cloud contours set from 0 to 2.0 g/kg with 0.5 g/kg interval, rain contours are set randomly with 5 contours per time step, the negative perturbation temperature chosen from the surface to the height of 250 m.

In the meantime, the wind shear triggering upward motion mostly appears at the level about ∼600 - 900 m above the surface during this most mature stage (Figure 10b). The updraft ascends in the opposite direction of the moving thunderstorm, particularly in front of the cloud storm indicates a typical of hailstorm formation in which this finding is consistent to the study of hailstorm evolution carried by *Chalon et al.* [1976] and *Chevuturi et al.* [2014]. The most forceful updraft reaches ∼25 m/s in the height of ∼13 km and produces the large graupel mass (8-10 g/kg) in the temperature between -15° and -45°C (Figure 11b), revealing that the hail formation occurs in this most intense stage.

However, the highest reflectivity in the low level (∼500 - 2000 m) corresponds to the area where rain mass mixing ratio appears instead of graupel (Figure 11b). This may imply that graupel shed with water is recognized as big raindrops instead of intact graupel by the model. As a result, although high reflectivity (40 - 60 dBz) appears, no graupel/hail sediments out at the surface area from this simulation. This finding agrees to *Stanford et al.* [2017] who found that a ubiquitous ice size bias on microphysics parameterization leads the model to produce high bias convective reflectivity for tropical deep convective cloud. The relatively moister air between 700 and 400 hPa (figure not shown) and the high freezing level (∼4.8 km) likewise can increase the melting of graupel as they fall. This CNTL also tends to release small latent cooling (figure omitted) in which creates warmer layer and weaker low-level cold pool (Figure 11c) compared to an idealized thunderstorm study carried by *Morrison and Milbrandt* [2010]. Thus, it is understandable that in this study model seems difficult to retain graupel particle in the surface layer.

Apart from the fact that this CNTL simulation fails to produce graupel/hail in the surface level, the dynamics and cloud microphysics of the thunderstorm are still well captured. Therefore, we can investigate the reason why the thunderstorm lasts longer over the urban area. The second intense stage is marked by the appearance of high reflectivity (40 - 45 dBz) in the low level atmosphere (0 - 2000 m) at 16.50 LST (Figure 10c). This figure shows that the retained sea breeze in the western part of the city seems able to create convergence area. The sea breeze front triggers the wind shear yet resulting a weaker upward motion than the first intense stage. The warm air parcel, facilitated by the low-level cold pool (Figure 11c), is lifted due to the high sensible heat flux over the city (figure not shown). For that reason, the hydrometeor production still appear in this stage but the number is lower (Figure 11c) compared to the previous intense stage. Hence, the longer lifetime of the intense stages can be concluded as the effect of retained sea breeze and warmer air which is indicated by the high UHI in the city (Figure 9). This finding agrees to *Yoshikado* [2017] who found that a sea breeze front remained over the city as a result of UHI effects. Finally, the cloud storm started to weaken as the sea breeze decays and the UHI slowly decrease due to rain chill the city (Figure 9). At 17.30 LST, the wind completely westerly in the low level (surface to 1.5 km height) and the rain area lasts only in the western part of Surabaya urban area (Figure 11d).

6 Influence of SST increase and urbanization to the thunderstorm intensity

As the sea breeze and urban-induced vigorous thunderstorm contribute to the 7$^{\text{th}}$ March 2017 hail event case, further investigation regarding urbanization and SST increase in Surabaya is performed. Factor separation is applied to examine how SST, building height, CCN concentration of urban aerosol, and their interactions influence the thunderstorm intensity. Despite that the CNTL only misses the graupel/hailstone at the surface, however, the thunderstorm dynamic and microphysics is well simulated. Therefore, in this section, the CNTL is chosen as the base run in which all the model simulations will be compared to. The used symbol on hereafter simulation is based on Table 2 and 3 in section 3. The analysis includes the upward motion, hydrometeor particle distributions, 6-h precipitation accumulation, and latent heat budget. Due to the complexity of the thunderstorm initiation and dynamic on each simulation, thus we only focus on the temporal and spatial analysis of those variables.

6.1 Influence of SST increase

The SH simulation adopts the single influence of the SST increase. Among other single factor influence, SST plays a main role in the thunderstorm intensity. The enhanced latent heating (Figure 16) triggers the upward motion reach up to 40 m/s. This stronger updraft contributes to the lifting of cloud droplet to the upper level of the atmosphere (Figure 12a). As a result, the urban-averaged of maximum graupel mass mixing ratio reach number of 7.5 g/kg (Figure 12a). Consequently, the cloud top is also higher than in the CNTL.

This SH simulation also shows that the increasing SST leads the formation of the thunderstorm earlier in time (Figure 12a). Since SST increases, the sea breeze circulation pattern remains the same but the strength becomes weaker due to the smaller gradient of temperature between land and ocean [*Kawai et al.*, 2006]. In consequence, the cloud will be easier to develop due to extra moisture supply ($\sim$0.5 g/kg) because of the

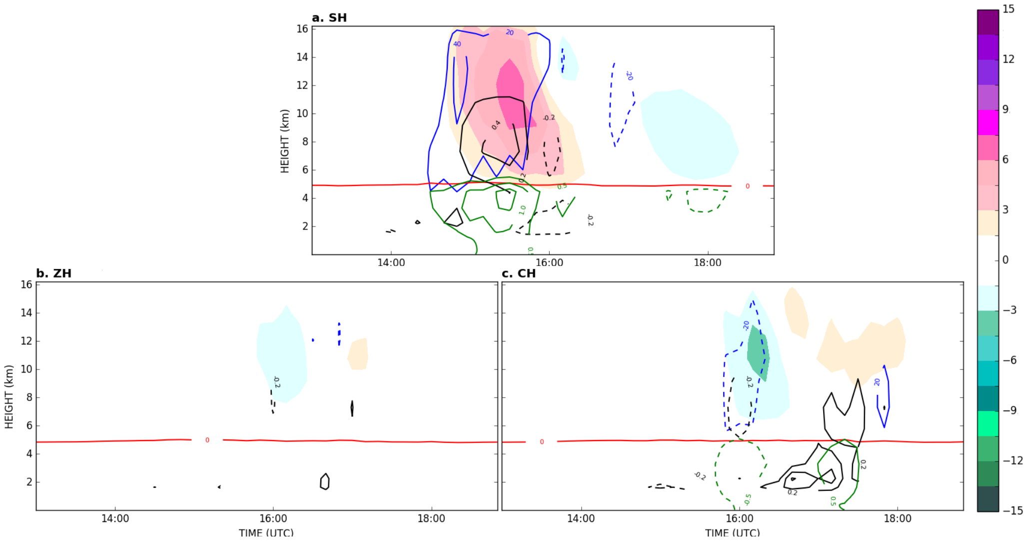

Figure 12. The difference field of simulated vertical temporal cross-section of graupel (shaded; g/kg), liquid water (black line; g/kg), rain (green line; g/kg), upward motion (blue line;m/s), and melting layer (red line; 0°C) between experiment and the CNTL for a. SH, b. ZH, and c. CH on 7th March 2017. The contour set from 0.2 to 0.8 g/kg at 0.2 g/kg interval, 0.5 to 2.0 g/kg at 0.5 g/kg interval, and 20 to 80 m/s at 20 m/s interval for cloud, rain, and upward motion respectively.

higher SST (not shown). Therefore, the first cloud initiation took place ∼1.5 hours earlier than the CNTL.

As the graupel mass mixing ratio increases, the rain mass tends to follow due to the ice particles melt below the freezing level. Yet, the most of the precipitation falls in the urban area when the SST increase (Figure 13a). This is because the moister air in the inland is closer to the urban area compared to the CNTL. However, the highest accumulated precipitation amounts to 45 mm and is more spotted at the location of the first cloud initiated and downwind area.

6.2 Influence of building height

The ZH simulation shows that the increased building height barely results in any differences of upward motion and hydrometeor particle distribution in the city. The CNTL and ZH simulation share the maximum graupel as well as the cloud mass (Figure 12b). However, the accumulated precipitation field ∼30% larger in the upwind area and the

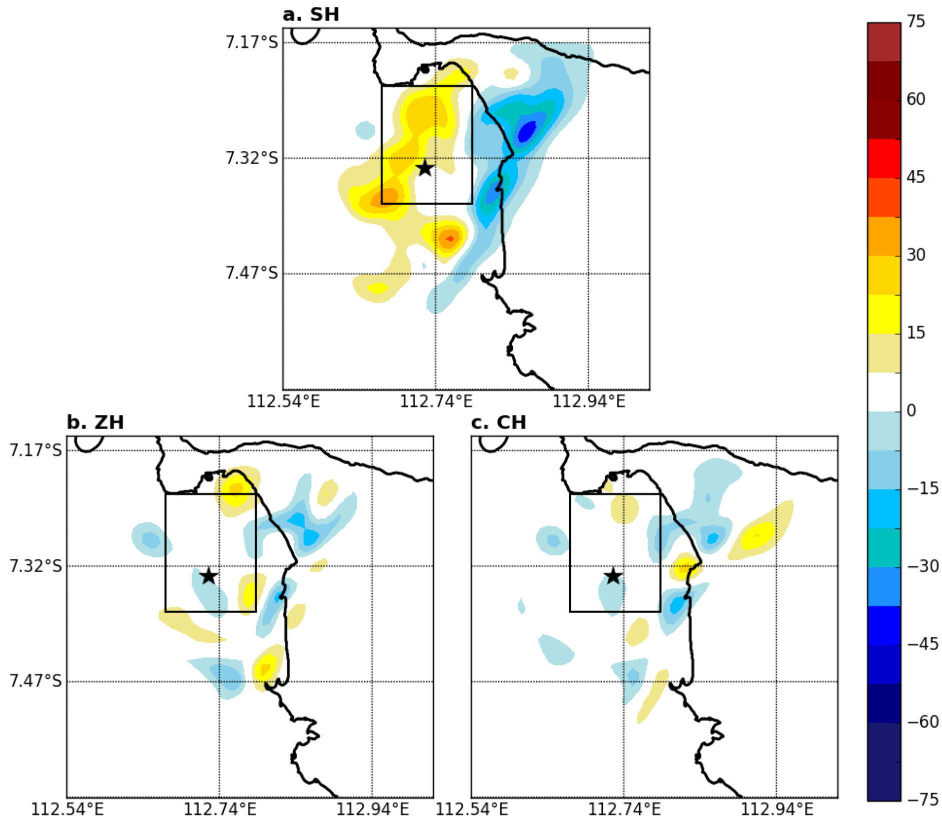

Figure 13. The difference field of simulated 6-h precipitation accumulation between experiment and the CNTL for a. SH, b. ZH, and c. CH. The rectangular black line indicates urban area while the black star shows the location hail reported on on 7$^{\text{th}}$ March 2017 from 13.00 to 19.00 LST.

urban side (Figure 13b). With increasing building height, the average wind speed in the city during the hail event is ∼0.5 m/s or ∼11% lower (figure omitted) which weakens the upward motion compared to the outside of the city because of the higher roughness effect of the urban area. As a result, the moving thunderstorm produces more scattered precipitation fields around the side of the city (Figure 13b) than in the city. The split cloud echoes due to the barrier effect (Figure 8g-h) also occur later (Figure 12b) and becomes stronger (Figure 13b) in the eastern part of the city (upwind area). Consequently, the precipitation is less in the city, particularly in the location where the hail event reported (Figure 13b). These findings agree to *Gunst* [2016]'s study who found that the building barrier effect in Houston, USA restricts the advection of convective precipitation so that decreased urban precipitation in the city.

6.3 Influence of CCN concentration of urban aerosol

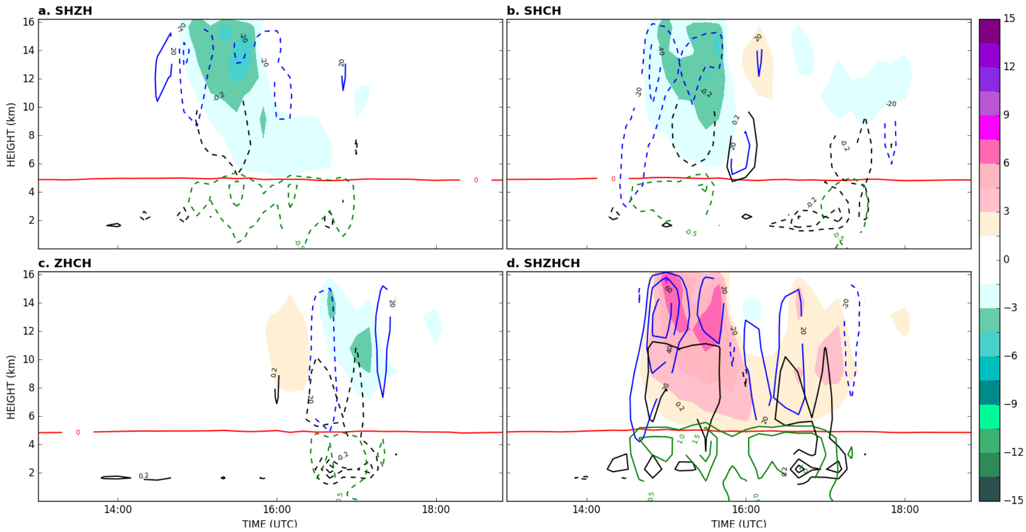

Figure 14. Same as in the Figure 12, but for interacted factors of a. SHZH, b. SHCH, c. ZHCH, and SHZHCH.

The single factor increasing of urban aerosol CCN concentration noted as the CH simulation. Although the maximum upward motion is similar (i.e ∼20 m/s), the maximum graupel mass is 1.5 g/kg or ∼33% lower over the urban area compared to the CNTL (Figure 12c). The small latent heating of this simulation above the freezing level can be the reason of the weakening ice formation over the city (Figure 16). In contrast with the SH simulation, in this CH simulation, the hydrometeor production comes later (Figure 12c). The reason for this later graupel and rain formation is 10-minutes delayed of the storm initiation. This because according to *Köhler* [1936] curve, in the same liquid water content, the more droplet on the cloud results the smaller droplet size in which more difficult to maintain. These findings also agree to the results of *Han et al.* [2012]'s study who found that higher concentration in the urban area delays raindrop formation due to the slow down of the diffusional cloud drops growth leads to the inefficient the collision-coalescence process in which takes longer on the raindrop formation.

Similar to the ZH simulation, in this CH simulation, the maximum of accumulated precipitation is 7.5 mm larger than the CNTL (Figure 13c). However, due to the slow westerly progress (not shown), most precipitation falls in the upwind area and only one spotted precipitation in the northern part of Surabaya urban area. With more CCN, less

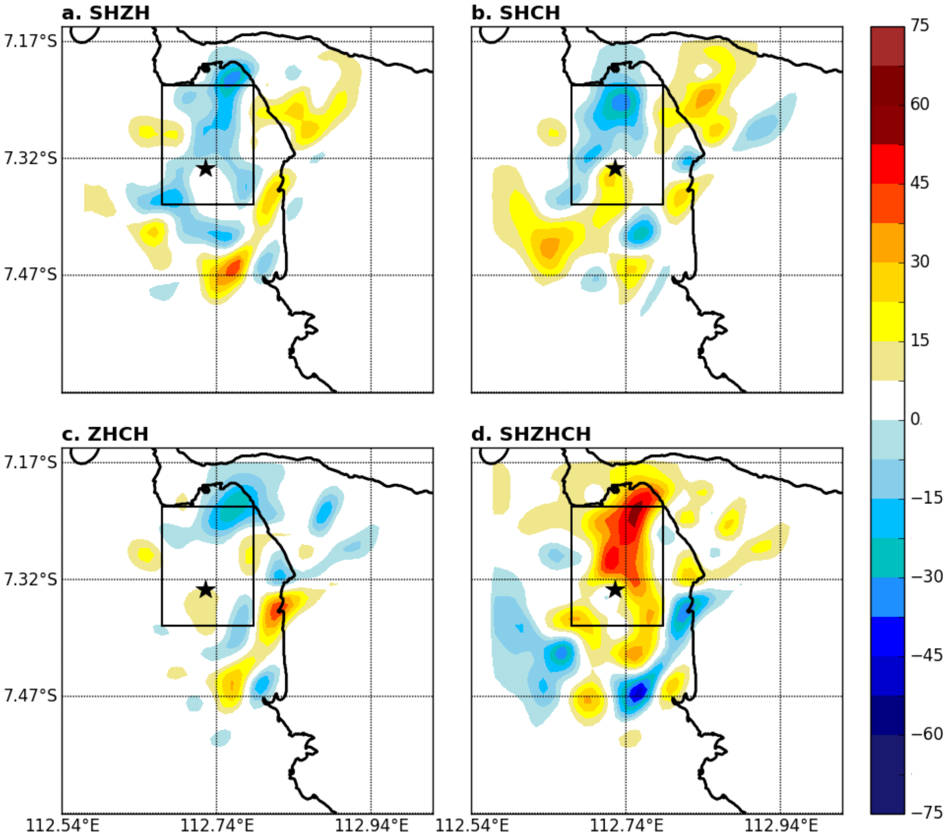

Figure 15. Same as in the Figure 13, but for interacted factors of a. SHZH, b. SHCH, c. ZHCH, and SHZHCH.

precipitation falls in the location of hail reported. It is because the CCN concentration does not influence the horizontal motion, therefore the wind speed remains same as the CNTL run which is lower than the observation (not shown).

6.4 Interaction among the factors

In reality it is difficult to just isolate individual factors to the urban-induced thunderstorm, thus in this section, we examine different interactions among the factors. The results show that the interactions among the factors greatly influence the accumulated precipitation. In all panels of Figure 15, the maximum 6-h accumulated precipitation tends to be larger 7.5 - 15 mm than the CNTL. It implies that both urbanization and SST increase has a contribution to the thunderstorm intensity in Surabaya urban area and its surrounding.

Nonetheless, the interaction between factors causes the thunderstorm's dynamics to differ from each other, in which results in a variation to the accumulated precipitation spatially. As the Figure 15a and 15b shows, the interactions where the SST contribute results wider rain area coverage compared to the CNTL. However, the feedback process between SST and CCN concentration is more prominent in the precipitation field (Figure 15b) than with the building height (Figure 15a). When SST variations are excluded, the area of accumulated precipitation is less and the maximum rain number is more scattered outside the city (Figure 15c). This is because the barrier effect of the increased building height forces the thunderstorm difficult to cross the city. Hence, the enhanced precipitation surrounding the urban area (upwind and side of the city in particular). It is not surprising that the modelled maximum graupel mass is less over the city when building height is increased (Figure 14a, 14c).

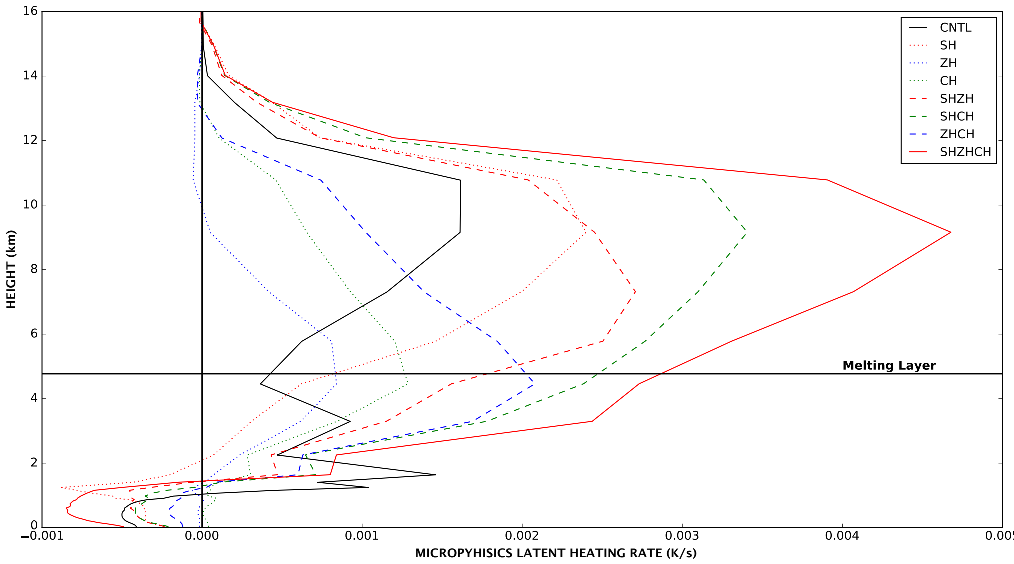

Figure 16. The Surabaya urban area and time-averaged of the vertical profile of difference field mean latent heating/cooling on the 7th March 2017 hail event case. Time-averaged from 13.00 to 19.00 LST. The colour and line style variation indicates the difference of factor influence.

Whilst, in the SHZHCH simulation, the enhanced thunderstorm intensity and accumulated precipitation becomes more prominent over the urban area (Figure 14d, 15d). The intensified of the latent heat release among three-factor interactions (Figure 16) trigger the updraft become three times stronger (from ∼20 to ∼60 m/s). The number of the hydrometeor production results in a longer thunderstorm lifetime than the CNTL and reaches 7.5 g/kg of maximum graupel mass mixing ratio (Figure 14d). It is because the SST increase with its additional moisture supply and the higher heat release due to the building height increase (not shown) initiates the thunderstorm earlier. However, this signal does not appear in two factors interacted, revealing a nonlinear contribution to this SHZHCH simulation. This suggests the presence of an additional/hidden factor which plays a significant role in this interactions. Thus, further physical analysis may be required to support this factor separation method in such cases as suggested by *Krichak and Alpert* [2002]who also found inconsistency of latent and sensible heat flux contribution to the cyclone development in eastern Mediterranean. Apart from the insufficiency of the factor separation method, it can be concluded that the SST increase is the main driver of thunderstorm development while the urbanization provides heat supply to enhance the thunderstorm intensity in the city (Figure 14 and 15).

To examine the influence of the urbanization on the thunderstorm intensity, one additional numerical simulation was performed in which the urban land-use changed to the cropland. The results showed that the replaced-urban area produced a shorter thunderstorm lifetime, a lower cloud top, and less accumulated precipitation compared to the CNTL. However, in this replaced-urban simulation, the thunderstorm can cross Surabaya urban area due to the absence of barrier effect. Consequently, the rain area is spotted in the Surabaya urban area (not shown).

7 Summary and conclusions

This study investigates the role of cloud microphysics, sea surface temperature (SST), and urbanization on the hail event simulation in Surabaya, Indonesia. The sensitivity of three cloud microphysics (Morrison-2, Thompson, and Goddard) and the use of urban canopy model were tested and compared to observations. Although simulation with combination of Morrison-2 and single urban canopy model underestimates the spatial extent of the rain area, the spatial structure corresponds to weather radar observation. It also exhibits suitable performance for the vertical atmosphere profile and the surface variables (i.e 2-m surface temperature, dew-point depression, 10-m wind speed and direction). Thus it is selected as a baseline run to carry out the two other study purposes; (i) to investigate the thunderstorm's physics and dynamics, (ii) to study the impact of the SST increase and urbanization on the location, timing, and intensity of the hail storm.

The control run worked reasonably well to simulate three stages of thunderstorms according to the time series of the maximum graupel mass on the averaged urban area. In the most intense stage, the stronger upward motion was triggered by the presence of the low-level convergence over the city. The UHI effect contributes to the urban-heat induced vigorous thunderstorm. This not only leads the hail formation but also retains the thunderstorm's lifetime longer due to the remained sea breeze front and warm air over the city.

In total, eight experiments have been conducted to study the influence of the urbanization and the increasing SST toward the thunderstorm intensity in the future. To distinguish the influence of the single factor and the interaction among them, the factor separation technique is used. Both urbanization and SST enhance the thunderstorm intensity in the urban area. Still, the SST is the main driver of moisture supply, followed by the CCN concentration and the building height. The sea breeze which promotes additional water vapour due to the SST increase supports cloud formation as the low-level convergence occurs. The raised CCN concentration due to urban pollution delays the graupel and rain formation because of the inefficiency of collision-coalesce process. Yet, the accumulated precipitation still increase in the upwind area. In spite of the enhanced accumulation precipitation is true for the building height increase, the barrier effect of this factor hinders the thunderstorm cross over the urban area.

When all factors are taken into account, the upward motion becomes three times stronger and graupel production is two times larger than in the reference run. This leads to a higher cloud top development and longer lifetime of the vigorous thunderstorm. Consequently, the accumulated rain becomes $\sim$15 - 30% larger, particularly in the western part of upwind area. However, nonlinear feedbacks among the factors suggesting a contribution of a hidden factor which is not well explained by factor separation method. Lastly, although the SST is the most contributory factor to the vigorous thunderstorm, yet the SST increase takes longer than the urbanization in the real world. Thus, a variety of urbanization factors (i.e urban fraction, urban size, anthropogenic heat release, etc.) await future work in investigating urban-induced hail event.

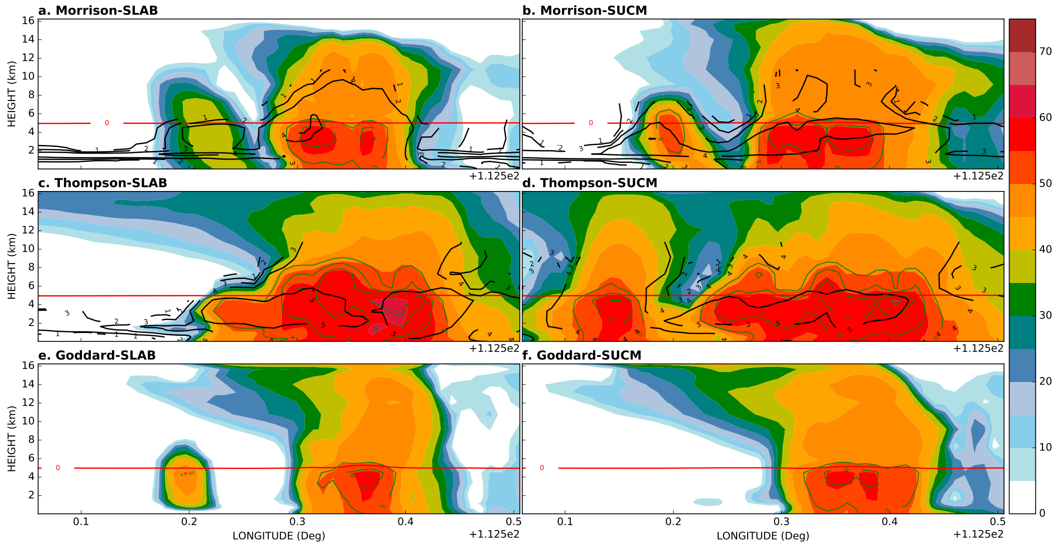

Figure A.1. Vertical cross section of reflectivity (shaded; dBz), rain mass mixing ratio (green; g/kg), total rain number concentration in base-10 logarithmic scale (black), and melting layer (red; °C) on averaged latitude of Surabaya urban area (7.2353° - 7.3885°S) for different ensemble scheme. The selected time based on averaged time when they reach the maximum reflectivity intensity. Noted that Goddard is a single moment scheme which only estimates mass mixing ratio.

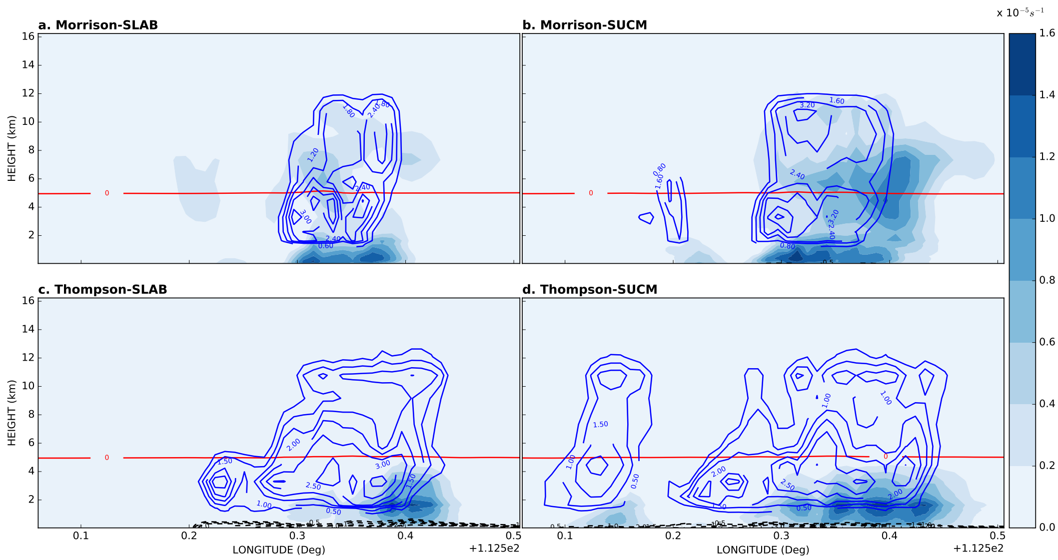

Figure A.2. Vertical cross section of evaporation rate (shaded; x $10^{-5}s^{-1}$), rain production (blue; x $10^{-5}s^{-1}$), perturbation potential temperature (θ') (dashed black; K), and and melting layer (red; °C) on same and time consideration as Figure A.1. The perturbation contours set from -3.0° to -0.5°C at -0.5°C interval. Area where the negative θ' appeared indicated as cold pool.

A: Cross-section analysis on different microphysics scheme

Acknowledgments

Thanks to all those who were involved in providing data and information on hail events in Surabaya, to Juanda Meteorological Station staffs in particular. The author also wishes to thank the Indonesia Endowment Fund for Education (LPDP) for the financial support and to Wageningen University staff that provide computer laboratory, assistance, and time discussion during this project.

References

Adams-Selin, R. D. and Ziegler, C. L. (2016). Forecasting hail using a one-dimensional hail growth model within WRF. *Mon. Weat. Rev.* 144, 4919–4939.

Alfieri, L., Claps, P., and Laio, F. (2010). Time-dependent ZR relationships for estimating rainfall fields from radar measurements. *Nat. Haz. Earth Sys. Sci.* 10, 149.

Ary, P. B. (2017).*Pesonal. Comm.* 2017-08-17.

Benjamin McBurney. (2015). Simulating the Sydney hailstomrs 9 December 2007 using WRF. *Master Thesis.* Macquarie Univ.

Bornstein, R. and Lin, Q. (2000). Urban heat islands and summertime convective thunderstorms in Atlanta: three case studies. *Atm. Env.* 34, 507–516.

Chalon, J. P., Famkhauser, J. C., and Eccles, P. J. (2008). Structure of an evolving hailstorm, Part 1: General characteristics and cellular structure. *Mon. Wea. Rev.* 104, 564–575.

Chatterjee, P., Pradhan, D., and De, U. K. (2008). Simulation of hailstorm event using mesoscale model MM5 with modified cloud microphysics scheme. *Ann. Geo.* 26, 3545–3555.

Chevuturi, A., Dimri, A. P., and Gunturu, U. B. (2014). Numerical simulation of a rare winter hailstorm event over Delhi, India on 17 January 2013. *J. Nat. Haz. and Earth Sys. Sci. (NHESS)* 14, 3331–3344.

Creighton, G., Kuchera, E., Adams-Sellin, R., McCormick, J., Rentschler, S., and Wickard, B.(2014). AFWA Diagnostic in WRF. *Tech. Rep.* Air Force Weather Agency, USA.

Dutsch, M. L. (2012). Evaluation of the WRF model based on observation made by controlled meteorological balloons in the atmosphere boundary layer of Svalbands. *Tech. Rep.* Meteorologisk Institutt.

Eusabio, A. S. (2017). Identifikasi Cuaca Ekstrim Hujan Es dan Angin Puting Beliung di Surabaya Tanggal 07 Maret 2017. *Unpublished Article.* BMKG Indonesia.

Gevorgyan, A. (2018). A case study of low-level jets in Yerevan simulated by the WRF model. *J. Geo. Res. Atm.*

Gunst, L. (2016). Urban Induced Precipitation over Houston, Texas and How It Is Controlled by Urban Heat, Surface Roughness, Building Height and Aerosol. *Master Thesis.* Wageningen Univ.

Halder, M., Hazra, A., Mukhopadhyay, P., and Siingh, D. (2015). Effect of the better representation of the cloud ice-nucleation in WRF microphysics schemes: A case study of a severe storm in India. *Atm. Res.* 154, 155–174.

Han, J. Y., Baik, J. J., and Khain, A. P. (2005). Microstimulation of the superior colliculus focuses attention without moving the eyes. *Proc. Natl. Acad. Sci. U.S.A.* 102, 524–529.

Hazra, A., Goswami, B. N., and Chen, J. P. (2013). Role of interactions between aerosol radiative effect, dynamics, and cloud microphysics on transitions of monsoon intraseasonal oscillations. *J. Atm. Sci.* 70, 2073–2087.

Hermawan, T. (2017). Analisa Cuaca Terkait Hujan Es di Surabaya Tanggal 7 Maret 2017. *Tech. Rep.* BMKG Indonesia.

Kawai, Y., Otsuka, K., and Kawamura, H. (2006). Study on Diurnal Sea Surface Warming and a Local Atmospheric Circulation over Mutsu Bay. *. 2* 84, 725–744.

Kilpeläinen, T., Vihma, T., Manninen, M., Sjöblom, A., and Jakobson, E., Palo, T., and Maturilli, M. (2017). Modelling the vertical structure of the atmospheric boundary layer over Arctic fjords in Svalbard. *Qua. J. Royal Met. Soc.* 138, 1867–1883.

Köhler, H. (1936). The nucleus in and the growth of hygroscopic droplets. *Trans. Faraday Soc.* 43, 1152–1161.

Krichak, S. O. and Alpert, P. (2002). A fractional approach to the factor separation method. *J. Atm. Sci.* 59, 2243–2252.

Kusaka, H., Kondo, H., Kikegawa, Y., and Kimura, F. (2001). A simple single-layer urban canopy model for atmospheric models: comparison with multi-layer and slab models. *Bound. Layer Met.* 101, 329–358.

Kusaka, H. and Kimura, F. (2004). Thermal effects of urban canyon structure on the nocturnal heat island: Numerical experiment using a mesoscale model coupled with an urban canopy model. *J. App. Met.* 43, 1899–1910.

Li, Dan, Bou-Zeid, E., Baeck, M. L., Jessup, S., and Smith, J. A. (2013). Modeling land surface processes and heavy rainfall in urban environments: Sensitivity to urban surface representations. *J. Hydromet.* 14, 1098–1118.

Lin, C. Y., Chen, W. C., Chang, P. L., and Sheng, Y. F. (2011). Impact of the urban heat island effect on precipitation over a complex geographic environment in Northern Taiwan. *J. App. Met. Clim.* 50, 339–353.

Luo, L., Xue, M., Zhu, K., and Zhou, B. (2017).Explicit prediction of hail using multimoment microphysics schemes for a hailstorm of 19 March 2014 in eastern China. *J. Geo. Res: Atm.* 122, 7560–7581.

Morrison, H., Curry, J. A., Shupe, M. D., and Zuidema, P. (2005). A new double-moment microphysics parameterization for application in cloud and climate models. Part II: Single-column modeling of Arctic clouds. *J. Atm. Sci.* 62, 1678–1693.

Morrison, H., and Milbrandt, J. (2010). Comparison of two-moment bulk microphysics schemes in idealized supercell thunderstorm simulations. *Mon. Wea. Rev.*

Orville, H. D. and Kopp, F. J. (1977). Numerical simulation of the life history of a hailstorm. *J. Atm. Soc.* 34, 1596–1618.

Papanastasiou, D. K., Melas, D., and Lissaridis, I. (2010). Study of wind field under sea breeze conditions; an application of WRF model. *Atm. Res.* 98, 102–117.

Pemerintah Surabaya (2014). Peraturan Daerah Kota Surabaya No. 12 Tahun 2014 Tentang Rencana Tata Ruang Wilayah Kota Surabaya Tahun 2014-2034. *Perda Surabaya.*

Pemerintah Surabaya (2014). Peraturan Walikota Surabaya No. 75 Tahun 2014 Tentang Pedoman Teknis Pengendalian Pemanfaatan Ruang Dalam Rangka Pendirian Bangunan di Kota Surabaya. *Perda Surabaya.*

M. Rajeevan1 , A. Kesarkar, M., Thampi, S. B., Rao, T. N., Radhakrishna, B., and Rajasekhar, M. (2010). Sensitivity of WRF cloud microphysics to simulations of a severe thunderstorm event over Southeast India. *Ann. Geophys.* 28, 603–619.

Rozoff, C. M., Cotton, W. R., and Adegoke, J. O. (2015). Simulation of St. Louis, Missouri, land use impacts on thunderstorms. *J. App. Met.* 42, 716–738.

Salanto, F. (2015). Research and Forecast Report: Surabaya Property Market Report 1st Half 2015. *Tech. Rep.* Colliers Int.

Sari, F. P. (2014). Pemanfaatan Model Weather Research Forecasting (WRF) untuk penentuan nilai ambang batas parameter cuaca dalam proses pertumbuhan awan cumulonimbus. *Bachelor Thesis.* STMKG Jakarta.

Sari, F. P. (2017). Effect of Different Microphysics Schemes on WRF Model: A Simulation of Hail event study case in Surabaya, Indonesia. *Unpublished Article.*

SELEX Sistemei Integrati. (2007). Instruction Manual Rainbow 5: Products and Alghoritms. *Manual Book*

Skamarock, W. C., Klemp, J. B., Dudhia, J., Gill, D. O., Barker, D. M., Wang, W., and Powers, J. G. (2005). A description of the advanced research WRF version 2. *Tech. Rep.* NCAR.

Sobirin and Fatimah, R. N. (2015). Urban Heat Island Kota Surabaya. *Geo Ed.* 4(2).

Stanford, Mc. W., Varble, A., Zipser, E., Strapp, J. W., Leroy, D., Schwarzenboeck, A., Potts, R., and Protat, A. (2017). A ubiquitous ice size bias in simulations of tropical deep convection. *Atm. Chem. Phy.* 17, 9599.

Stein, U. and Alpert, PINHAS. (1993). Factor separation in numerical simulations. *J. Atm. Sci.* 50, 2107–2115.

Stensrud, D. J., Coniglio, M. C., Knopfmeier, K. H., and Clark, A. J. (2015). Numerical Models: Model Physics Parameterization. *Enc. Atm. Sci. (Sec. Ed.)* 2, 167–180.

Tao, W. K., Simpson, J., Baker, D., Braun, S., Chou, M. D., Ferrier, B., Johnson, D., Khain, A., Lang, S., Lynn, B., and others. (2016). Microphysics, radiation and surface processes in the Goddard Cumulus Ensemble (GCE) model. *Met. Atm. Phy.* 82, 97–137.

Taruna, R. M., Zakir, A., and Permata, C. A. D., and Farareta, L. (2016). Analisis CAPE dan K-Indeks terhadap Prediksi Awan Cumulonimbus dan Badai Guntur di Surabaya Periode 2010 - 2014. *Prosiding Seminar HMD 2016.* STMKG, 96–108.

Thompson, G., Field, P. R., Rasmussen, R. M., and Hall, W. D. (2008). Explicit forecasts of winter precipitation using an improved bulk microphysics scheme. Part II: Implementation of a new snow parameterization. *Mont. Wea. Rev.* 136, 5095–5115.

Tjiptoherijanto, P. (1999). Urbanisasi dan Pengembangan Kota di Indonesia. *Populasi* 10(2).

Tresnawati, M. (2016). Kajian hujan es di Surabaya (Studi kasus tanggal 20 Februari 2014, 9 Desember 2014, dan 20 Februari 2015. *Bachelor Thesis.* STMKG Jakarta.

Yang, H., Xiao, H., Guo, C., Wen, G., Tang, Qi, and Sun, Yue (2017). Comparison of aerosol effects on simulated spring and summer hailstorm clouds. *Adv. in Atm. Sci.*34, 877–893.

Yoshikado, H. (2017). Interaction of the sea breeze with urban heat islands of different sizes and locations. *J. Met. Soc. Japan. Ser. III* 72, 139–143.

Zhang, Y, Miao, S., Dai, Y., and Bornstein, R.(2017).Numerical simulation of urban land surface effects on summer convective rainfall under different UHI intensity in Beijing. *J. Geo. Res. Atm.* 122, 7851–7868.

Zipser, E. J., Liu, C., and Cecil, D. J., Nesbitt, S. W., and Yorty, D. P.(2006). Where are the most intense thunderstorms on Earth?. *Bul. of the American Met. Soc.* 87, 1057–1071.